1988

Epitrochoidal Versus Hypotrochoidal Gerotor Type Pumps With Special Attention to Rubbing Velocities

John E. Beard
Louisiana State University

Moreover, the refrigerating capacity becomes fixed after the start of capacity control. As for these results, the torque Tr started a drop at $N \geq 1800$ rpm, and at $N = 5000$ rpm, in constant to the value of $N = 1800$ rpm, about a 35% reduction was reached.

Consequently, with a system employing a capacity control compressor there is no attachment and detachment of the electromagnetic cluth in the range of capacity control, so a stable value with no fluctuation is maintained, thus yielding comfortable temperature regulation and driving feeling (See Fig. 12)

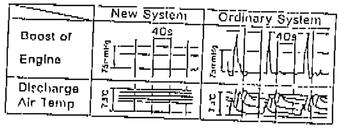

Fig. 12 Comparison of fluctuations

CONCLUSIONS

In the development a vane rotary type capacity control compressor equipped with a capacity control mechanism which engaged the method of automatically delaying the ending position of suction process, we studied dynamic behavior of capacity control mechanism and came to the following conclusions.

1. The control mechanism using a arc-shaped slider is simple, with few additional parts and enables capacity control over the wide range from 10 to 100%.
2. At the refrigerating cycle employed the capacity control compressor, with pressure control valve which stabilize suction pressure constant, refrigerating capacity becomes constant after the start of capacity control, and reduction of compressor torque is reached. Consequently yielding comfortable temperature regulation and driving feeling with no fluctuation in the range of capacity control.
3. Through analysis of capacity control compressor, results of theoretical analysis tend to agree with experimantal one and the methods we employed can establish outstanding control responce and stability characteristics.

NOMENCLATURE

A_1 : Pressure reception area of Diaphragm
A_2 : Pressure reception area of Steal ball
A_3 : Pressure reception area of Slider
C : Flow rate coefficient
d_2 : Diameter of outlet hole from pressure control valve
d_3 : Diameter of outlet hole from pressure control chamber
Fi : Sum of initial spring strengths of spring (1) and (2)
F_3i : Initial spring strength of spring (3)
F_3 : Side pressure applied to slider
g : Gravitational acceleration
Ko : Gain constant of Refrigerating cycle
k_1 : Spring constant of spring (1)
k_2 : Spring constant of spring (2)
k_3 : Spring constant of spring (3)
M_3 : Mass of Slider
N : Compressor rotation speed
No : Compressor rotation speed at control start
Pa : Atmospheric pressure
Pc : Critical pressure ratio

P_d : Compressor discharge pressure
P_H : High pressure
P_m : Pressure of pressure control chamber
P_s : Suction pressure of Compressor
Q_e : Refrigerating capacity
Q_1 : In-flow rate to pressure control chamber
Q_2 : Out-flow rate from pressure control chamber
R_3 : Flow resistance of slider side gap
T_o : Reponse time coefficient of Refrigerating cycle
T_r : Compressor required torque
V : Volume of cylinder chamber
V_{th} : Maximum theoretical volume of cylinder chamber
X_1 : Lift of steel ball
X_3 : Displacement of Slider
ε : Compression ratio
γ_H, γ_m : Gas specific weight
μ : Friction coefficient
κ : Specific heat ratio
η_v : Volumetric efficiency of Compressor
η_{v0} : Volumetric efficeincy of Compressor at control start

REFERENCE

1. J. Reichelt, et al., "REFRIGERATING COMPRESSORS FOR AIR CONDITIONING OF PASSENGER CARS." Purdue Compressor Technology Conference, July 1986, pp 537-549
2. T. Maruyama, et al., "CAPACITY CONTROL OF ROTARY TYPE COMPRESSORS FOR AUTOMOTIVE AIR-CONDITIONERS" Purdue Compressor Technology Conference, July 1982, pp 284-291
3. Timothy J. Skinner, et al., "V-5 AUTOMOTIVE VARIABLE DISPLACEMENT AIR CONDITIONING COMPRESSOR" SAE 850040, Feb. 1985
4. Yoji Nishimura, et al., "DEVELOPMENT OF TWO-STAGE VARIABLE DISPLACEMENT COMPRESSOR FOR AUTOMOTIVE AIR CONDITIONER" SAE850039, Feb. 1985
5. H. Holdack-Janssen, et al., "CONTINUOUS AND DISCONTINUOUS CAPACITY CONTROL FOR HIGH SPEED REFRIGERATION COMPRESSORS" Purdue Compressor Technology Conference, July 1986 pp 67-75

THE ANALYSIS OF DIMENSIONAL COMMONIZATION PROCEDURES CONSIDERING THE EFFICIENCY FOR THE ROLLING PISTON COMPRESSORS

Caio Franco da Costa
EMBRACO - Empresa Brasileira de Compressores S/A
P.O. Box D-27 - 89200 Joinville - SC - Brazil

ABSTRACT

The present work deals with dimensional commonization procedures and their different effects over the performance of the compressor. The study is made theoretically with the use of a previously validated simulation program at a refrigeration compressor series with capacity range from 650 to 1000 Btu/hr.

Efficiency is analysed through graphs showing the variation of the energy efficiency ratio (EER), capacity and power consumption over the swept volume domain, for each of the commonization alternatives. The results of the energetic and the volumetric efficiency over the swept volume domain are also shown.

Furthermore, in order to get a detailed understanding of the said processes, each specific energy and mass loss causing the capacity and consumption variations are also disclosed in graphs.

INTRODUCTION

Dimensional commonization procedures are meant primarily as a way to attain process simplification and consequently cost reduction. However such procedures must also be considered in terms of the resulting performance and efficiency of the compressor.

The displacement of a rolling piston compressor is given basically by its three main dimensions: cylinder diameter, cylinder height and roller diameter. Therefore there are three possible commonization procedures for the parts in the same compressor series; obtained by changing singly one dimension keeping the two others constant.

The present work deals, with the commonization procedures and their different effects over the efficiency of the compressor.

COMMONIZATION PROCEDURES

As mentioned above there are three direct dimensional commonization procedures for any group of pumping kits of rolling piston compressors of the same series. Also a fourth procedure, a derivation, will be examined (see table 1).

The first, and most elementary procedure [≠ H], is to change the height of the cylinder (H) keeping every other dimension constant. The second type of procedure [≠ Ør, = Øe] is to change the roller diameter (Ør), and consequently the eccentricity of the shaft (Ec), keeping constant the cylinder height, cylinder diameter (Øc) and, particulary, the eccentric journal diameter (Øe), hence, shifting also the roller thickness (tr). The third procedure [≠ Ør, ≠ Øe], a variation of the second one, is achieved changing the roller diameter and the shaft eccentricity yet altering also the eccentric journal diameter, so that the roller thickness is kept constant for all kits in the group. The fourth possible commonization [≠ Øc], is to change the cylinder diameter and the eccentricity, keeping constant every other dimension.

The consequences of each of these commonization procedures in the manufacturing process can be easily deduced by those skilled in the art by examining table 2, where the commonization of a group of "n" compressor kits is shwon. As the manufacturing process analysis would be out of the scope of this work, we will not make any further consideration on this matter.

COMMONIZATION PROCEDURES AND COMPRESSOR EFFICIENCY

To analyze theoretically the effects of the dimensional commonization procedures on the compressor efficiency we made use of a previously validated simulation model (1). A hypothetical series of compressors with displacement within the range of 4.0 to 6.1 cc, the most standard range in the refrigeration market, were chosen to be simulated under the four commonization procedures, on the -23.3/54.4°C condition.

The commonizations were made considering the dimensions found for the medium swept volume (Vs) of the range as the leading dimensions, i.e. the dimensions kept constant for each compressor kit of each different commonization procedure were those calculated for the medium swept volume of the range (see example in table 3).

Figure 1 presents the results found in the EER for the four commonization procedures*. As the graph shows the [≠ H] procedure gives the most constant EER within the range, and the [≠ Ør,≠ Øe] procedure gives the highest EER slope. It is interesting to point that no matter where the leading Vs is chosen between the range, the rank of the slopes of the lines for the four procedures will not be altered. Another important issue is that the better procedure to be chosen depends on if the original existing kit (leading kit) has whether a greater or a smaller volume than the derived ones. That is, if the original existing kit is smaller than the derived ones, still to be designed, the best procedure, in terms of efficiency, would be the [≠ Ør, ≠ Øe] procedure. On the contrary, if the original kit has a greater volume than those to be derived the best choise would be the [≠ H] procedure, for the higher EER.

Figures 2a and 2b present the volumetric efficiency (ηv)and the energetic efficiency (ηe) over the swept volume domain for the four commonization procedures. It can be noted that for the ηe the rank of the slopes of the lines is the same of that of the EER lines, but for the ηv three of the procedures show almost the same line and the [≠ H] procedure has a much lower slope than the others. It means that the EER is much more a result of the ηe than the ηv variance.

To understand in detail the reasons for each different procedure behavior it is necessary to take a close look on the variations of the energy and mass losses. In order to simplify this study the analysis is made only from the medium (5.09 cc) up to the greater swept volume. For the left side of the graphs the analysis should be made reversely.

The gas leakage through the minimum clearance between the roller and the cylinder walls (Fig 3a) is mainly a function of the cylinder height, what explains its sharp increase for the [≠ H] procedure. On the other hand the gas leakage through the vane edges (Fig 3b) is almost constant for the [≠ H] procedure, because this leakage is a function mainly of the eccentricity which does not change for the [≠ H] procedure. While for the other three procedures this leakage will have a almost constant increase with the eccentricity.

The vane tip friction loss (Fig 3c) is also mainly a function of the cylinder height, hence, the analysis is similar to that made for the lines of the graph on Figure 3a.

The friction loss between the roller and the eccentric journal (Fig 3d) is a function of the cylinder height, hence it has a great increase for the [≠ H] procedure. On the contrary for the [≠ Ø, ≠ Øe] procedure this loss drops because its also a function of the eccentric journal diameter which, for this case, decreases with the volume. While for the other two procedures it is constant because there is no change in neither cylinder height or eccentric journal diameter.

The friction loss caused by the slinding of the vane inside the cylinder slot (Fig 3) is mainly a function of the sliding velocity and the gas force along the vane sides so that the lines will respond for a combination of the eccentricity of the shaft and cylinder height.

The energy loss caused by the admission of the hot oil into the cylinder through the roller faces and the vane sides, increasing the refrigerant gas temperature, specially in the suction volume, is called oil heating loss (Fig 3f).

* The values shown in the next figures (except Figs 2) are relative values to those obtained for the leading kit (Vs = 5.09 cc), see table 4.

It suffers a great increase for the [≠ H] and the [≠ Ør, = Øe] procedures. In the first because the oil leakage through vane sides is proportional to the cylinder height, in the latter because the oil admitted through the roller faces is inversely proportional to the roller thickness. While for the [≠ Ør, ≠ Øe] procedure there will be a small decrease in the oil heating loss due to the decrease in the roller medium perimeter, what is characteristic of this procedure. For the [≠ Øc] procedure both height and roller medium perimeter are kept constant so that the oil heating loss is almost constant.

CONCLUSION

The efficiency of the rolling piston compressor, for each of the four possible dimensional commonization procedures were examined. The best procedure to be chosen depends on the swept volume of the original existing kit relative to the volumes of those kits still to be design. In case the new kits have smaller volumes than the original one the best choice for the higher efficiency would be the [≠ H] procedure. If the new kits have greater volumes than the original one the best procedure is the [≠ Ør, ≠ Øe] procedure. In case a whole new series of kits is to be designed from a medium volume leading kit the [≠ H] procedure would give the most constant efficiency slope. Those considerations are made only in terms of efficiency.

REFERENCES

1 - COSTA, C. F. - "Use of a Simulation Model for Theoretical Optimization Analysis of a Rolling Piston Type Compressor", ICEC, Purdue University (1986).

2 - COATES, D. A. - "Performance Improvement and Dimensional Commonization with a Compressor Simulation", PCTC, Purdue University (1972).

Types	H	Øc	Ør	Ec	Øe	tr
[≠ H]	≠	=	=	=	=	=
[≠ Ør, = Øe]	=	=	≠	≠	=	≠
[≠ Ør, ≠ Øe]	=	=	≠	≠	≠	=
[≠ Øc]	=	≠	=	≠	=	=

Table 1: Types of Dimensional Commonization Procedures.

Commonization Types	Number of Parts			Number of Different Dimensions				
	Cylind.	Roller	Shaft	H	Øc	Ør	Ec	Øe
[≠ H]	n	n	n	n	1	1	1	1
[≠ Ør, = Øe]	1	n	n	1	1	n	n	1
[≠ Ør, ≠ Øe]	1	n	n	1	1	n	n	n
[≠ Øc]	n	1	n	1	n	1	n	1

Table 2: Types of Dimensional Commonization and Manufactured Parts for a group of "n" kits.

Vs (cc)	H (mm)	Øc (mm)	Ør (mm)	Ec (mm)	Øe (mm)	tr (mm)
4.07	16	40	35.7	2.14	23	6.36
4.58	16	40	35.1	2.42	23	6.07
5.09	16	40	34.6	2.72	23	5.78
5.59	16	40	34.0	3.00	23	5.49
6.10	16	40	33.4	3.31	23	5.19

Table 3: Example of Dimensional Comonization for the [≠ Ør, = Øe] procedure (group of 5 kits).

Volumetric Losses	% of mass flow
. Minimum clearance leakage	4.28
. Vane edges leakage	1.15
Energy Losses	**% of power input**
. Vane tip friction	1.63
. Roller/eccentric friction	2.50
. Vane/slot friction	1.89
. Oil heating	5.14

Table 4: Volumetric and Energy Losses for the Leading Kit (Vs = 5.09 cc).

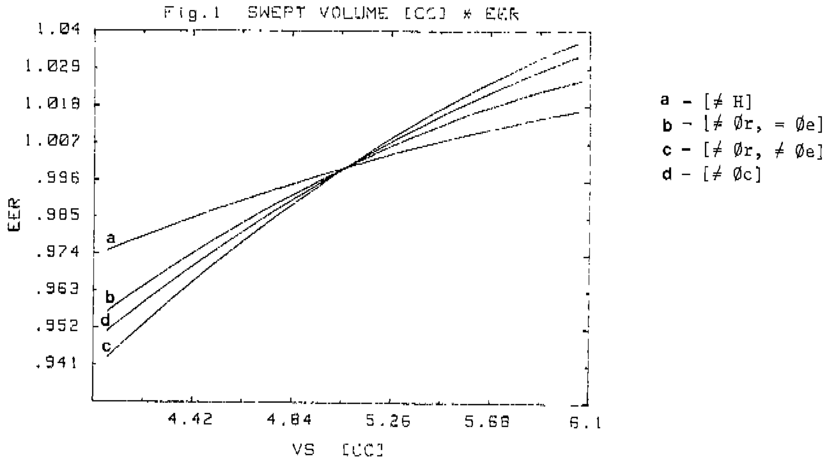

Fig.1 SWEPT VOLUME [CC] * EER
1.04
1.029
1.018
1.007
.996
.985
.974
.963
.952
.941
EER
a
b
d
c
4.42
4.84
5.26
5.68
6.1
VS [CC]
a - [≠ H]
b - [≠ Ør, = Øe]
c - [≠ Ør, ≠ Øe]
d - [≠ Øc]

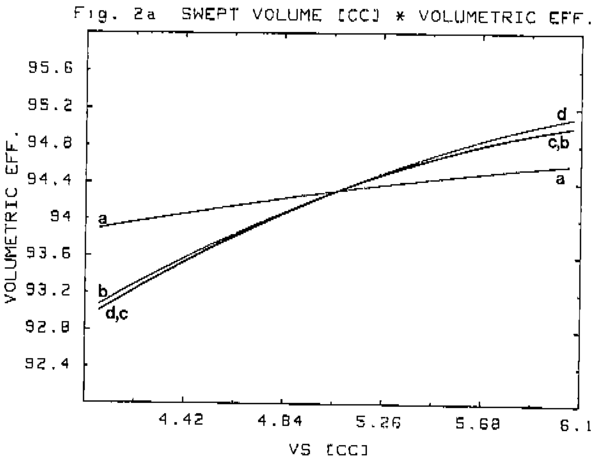

Fig. 2a SWEPT VOLUME [CC] * VOLUMETRIC EFF.
95.6
95.2
94.8
94.4
94
93.6
93.2
92.8
92.4
VOLUMETRIC EFF.
d
c,b
a
a
b
d,c
4.42
4.84
5.26
5.68
6.1
VS [CC]

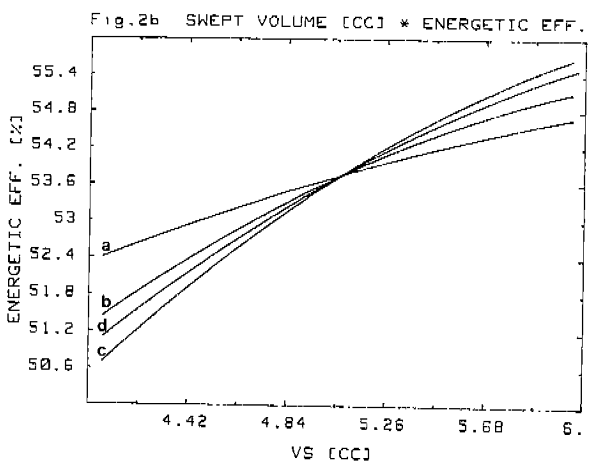

Fig.2b SWEPT VOLUME [CC] * ENERGETIC EFF.
55.4
54.8
54.2
53.6
53
52.4
51.8
51.2
50.6
ENERGETIC EFF. [%]
a
b
d
c
4.42
4.84
5.26
5.68
6.1
VS [CC]

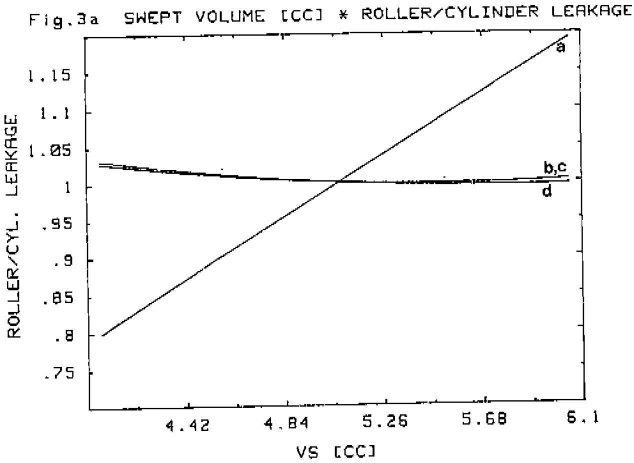
Fig.3a SWEPT VOLUME [CC] * ROLLER/CYLINDER LEAKAGE
ROLLER/CYL. LEAKAGE
1.15
1.1
1.05
1
.95
.9
.85
.8
.75
4.42
4.84
5.26
5.68
6.1
VS [CC]
a
b,c
d

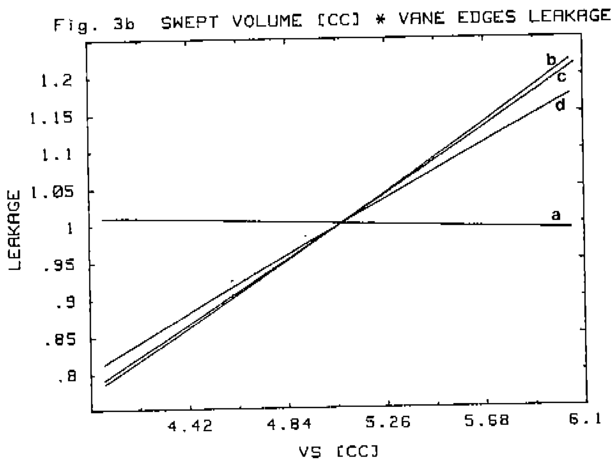
Fig. 3b SWEPT VOLUME [CC] * VANE EDGES LEAKAGE
LEAKAGE
1.2
1.15
1.1
1.05
1
.95
.9
.85
.8
4.42
4.84
5.26
5.68
6.1
VS [CC]
b
c
d
a

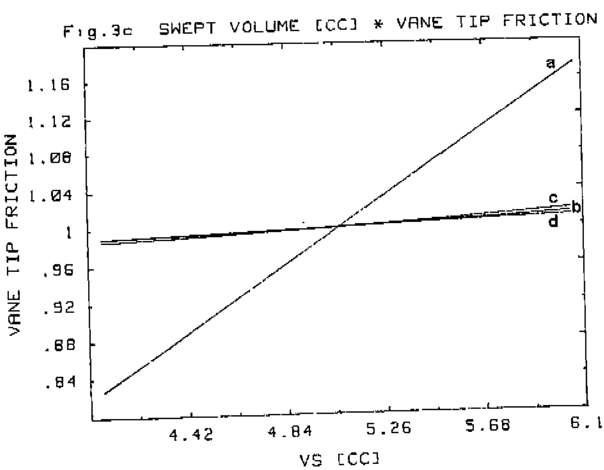
Fig.3c SWEPT VOLUME [CC] * VANE TIP FRICTION
VANE TIP FRICTION
1.16
1.12
1.08
1.04
1
.96
.92
.88
.84
4.42
4.84
5.26
5.68
6.1
VS [CC]
a
c
b
d

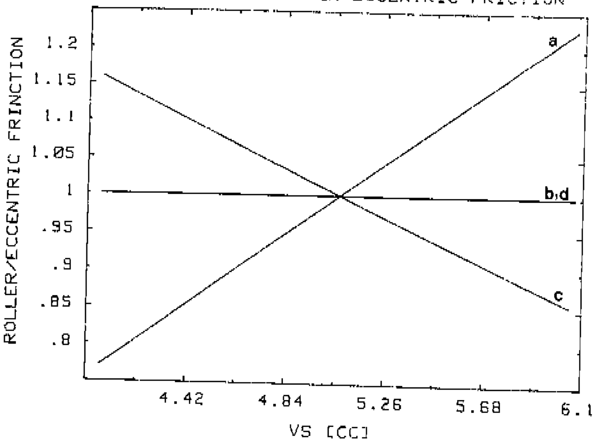
Fig.3d VS * ROLLER/ECCENTRIC FRICTION
ROLLER/ECCENTRIC FRINCTION
1.2
1.15
1.1
1.05
1
.95
.9
.85
.8
a
b,d
c
4.42
4.84
5.26
5.68
6.1
VS [CC]

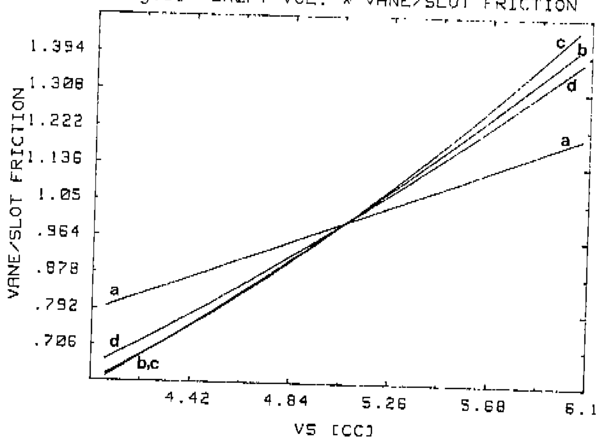
Fig.3e SWEPT VOL. * VANE/SLOT FRICTION
VANE/SLOT FRICTION
1.394
1.308
1.222
1.136
1.05
.964
.878
.792
.706
c
b
d
a
a
d
b,c
4.42
4.84
5.26
5.68
6.1
VS [CC]

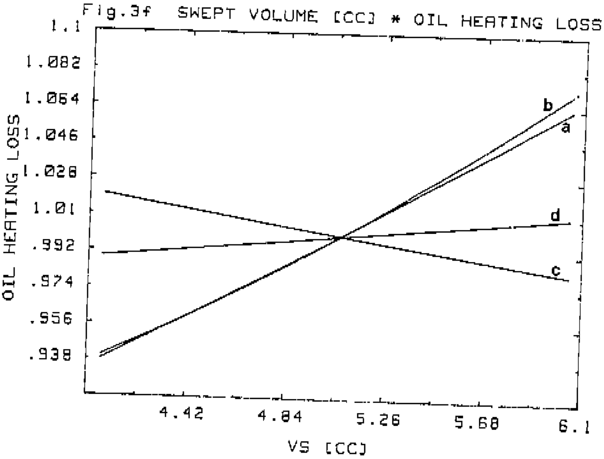
Fig.3f SWEPT VOLUME [CC] * OIL HEATING LOSS
OIL HEATING LOSS
1.1
1.082
1.064
1.046
1.028
1.01
.992
.974
.956
.938
b
a
d
c
4.42
4.84
5.26
5.68
6.1
VS [CC]

EPITROCHOIDAL VERSUS HYPOTROCHOIDAL GEROTOR TYPE PUMPS WITH SPECIAL ATTENTION TO RUBBING VELOCITIES

John E. Beard, Assistant Professor
Louisiana State University
Department of Mechanical Engineering
Baton Rouge, Louisiana

Abstract

The planar rotary mechanism, by virtue of its volume changing ability can be used as a pump, engine or compressor. The rubbing velocity is the relative velocity between the points of contact of the two working chambers. The rubbing velocity of the planar rotary mechanism, commonly known as a gerotor, influences the wear rates and heat transfer rates. This paper presents the effects of design parameters on the rubbing velocity for epitrochoidal and hypotrochoidal gerotors and the rubbing velocity versus displacement.

INTRODUCTION

The first practical rotary mechanism, commonly known as the gerotor has been used successfully for a pump since the 1920's. The gerotor is usually used as a pump although the Wankel engine, a gerotor, has had limited success as an internal combustion engine and is now obtaining increasing usage as a compressor.

Leemhius [1] presented the rubbing velocity (apex velocity) for epitrochoidal generated gerotors where the generating pin has zero diameter. Colbourne [2] presented a method to determine the evelopes of trochoids which are generated by planetary motion. Hall [3] presented the mathematics necessary to determine the minimum radius of curvature on the generated shape by the trochoidal motion. Colbourne [4] presented the theoretical flow rate of epitrochoidal type gerotors and the effect of the shape of the generating arc on the flow rate. Beard [5] varied the radius and location of the generating circular arc to determine its effect on the flow rate and pocket displacement. Beard [6] presented the effects of the design parameters on the volume change ratio and size for hypotrochoidal and epitrochoidal gerotors. Beard [7] presented the effects of the design parameters on the rubbing velocity of the epitrochoidal gerotor.

It is belived that the relationships for the rubbing velocities for the epitrochopidal versus hypotrochoidal gerotors have not been previously presented. Since the rubbing velocity (apex velocity) for epitrochoidal and hypotrochoidal gerotors is of concern when designing gerotors the effects of the design parameters on the rubbing velocity versus displacement for both epitrochoidal and hypotrochoidal gerotors are presented.

MATHEMATICAL DEVELOPMENT

Epitrochoidal Motion of the Generating Arc

To generate a gerotor, where the center of the path of the generating circular arc creates an epitrochoid, the generating arc is placed on the larger circle of radius r_2 and this circle is rolled without slipping on the smaller circle of radius r_1, Figure 1. Points q_1 and $q\prime$ are the points nearest and furthest from the instant center and their paths generate the gerotor. To

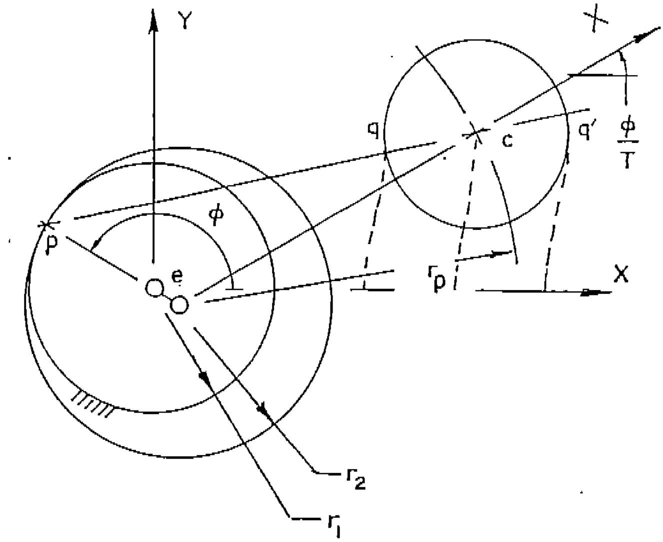

Figure 1: Epitrochoidal path of the generating pin center plus the generated portion of inner and outer envelope

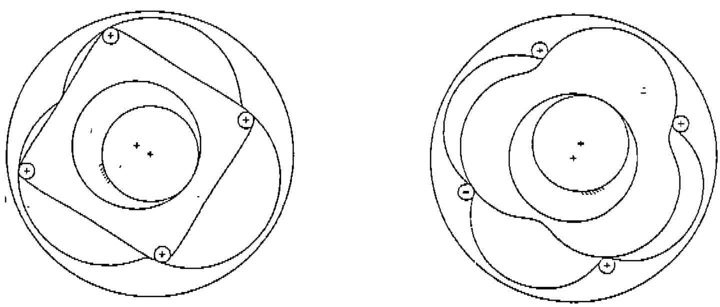

(a) External Contact

(b) Internal Contact

Figure 2: Epitrochoidal generation

generate complete closed curves the following ratio of radii is used.

$$r_1 = r_2(T-1)/T \tag{1}$$

Where T and $T-1$ are lobes or teeth on the generating and generated shape respectively. Figures 2a and 2b are examples of gerotors that can be contained in the same envelope, have the same $T/(T-1)$ ratio, were generated with a generating arc of r at a distance r_p from the center of the circle containing the generating arc. The rubbing velocity between the moving and fixed gear is determined by the following equations when the center of the generating circular arc follows an epitrochoidal path.

$$V_q = \omega * pq \tag{2}$$

$$V_{q'} = \omega * pq' \tag{3}$$

where ω is the angular velocity of the moving gear and is equal to:

$$\omega = \frac{\dot{\phi}}{T} \tag{4}$$

Since the angular velocity of the moving gear is a linear function of the angular velocity of the arm, for simplicity $\dot{\phi}$ will be set equal to one for all calculations. The distance to the center of the generating pin from the instant center between the fixed and moving gear is:

$$pc = \sqrt{r_P{}^2 + r_2{}^2 - 2.0 r_2 r_P cos(\phi(1 - 1/T))} \tag{5}$$

therefore

$$pq = pc - r \tag{6}$$

and

$$pq' = pc + r \tag{7}$$

The contained pocket area is presented without derivation and its development can be found in reference 4.

$$\frac{dA}{d\phi} = \frac{4 r_2 r_p sin(\frac{\phi}{T})}{T-1} \tag{8}$$

$$\pm \frac{r}{T} \int_{\frac{\pi}{T-1}}^{\frac{\pi(T+1)}{T-1}} \sqrt{r_P{}^2 + r_2{}^2 - 2.0 r_2 r_P cos(\phi(1 - 1/T))} \tag{9}$$

$$- \sqrt{r_P{}^2 + r_2{}^2 - 2.0 r_2 r_P cos(\frac{2\pi}{T} - \phi(1 - 1/T))}\, d\phi \tag{10}$$

The $\pm$ are the displacements for the external and internal contact respectively. Beard [6] determined that the radius of the generating pin, r , has little effect on the flow rate or displacement. By using the following value of r a direct comparison between the internal and external contact gerotors can be made.

$$r = \frac{r_2}{2\,T} \tag{11}$$

Hypotrochoidal Motion of the Generating Arc

To generate a gerotor, where the center of the path of the generating circular arc creates an hypotrochoid the generating arc is placed on the smaller circle of radius r_1 and this circle is rolled without slipping on the larger circle of radius r_2, Figure 3. Points q_1 and q' are the points nearest and furthest from the instant center and their paths generate the gerotor. To generate complete closed curves for both epitrochoidal and hyptrochoidal gerotors the ratio given in equation one is used. The rubbing velocity between the moving and fixed gear is determined in the same manner as the epitrochoidal gerotor.

$$V_q = \omega * pq \tag{12}$$

$$V_{q'} = \omega * pq' \tag{13}$$

where ω is the angular velocity of the moving gear and is equal to:

$$\omega = -\frac{\dot{\phi}}{T-1} \tag{14}$$

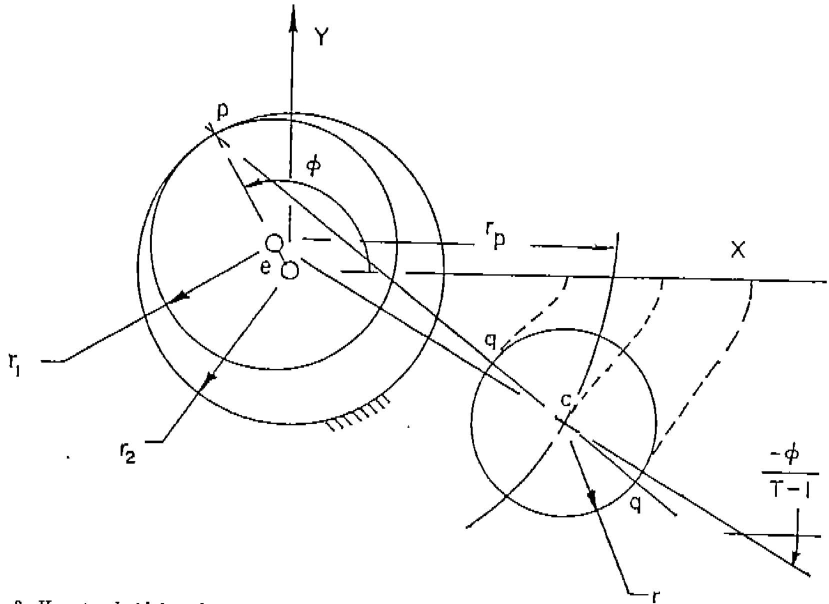

Figure 3: Hypotrochoidal path of the generating pin center plus the generated portion of inner and outer envelope

As in the case of the epitrochoidal gerotor the angular velocity of the moving gear is a linear function of the angular velocity of the arm and will be set equal to one for all calculations. The distance to the center of the generating pin from the instant center between the fixed and moving gear is:

$$pc = \sqrt{r_P{}^2 + r_1{}^2 - 2.0 r_1 r_P cos(\phi(T/(T-1))} \tag{15}$$

with

$$pq = pc - r \tag{16}$$

and

$$pq\prime = pc + r \tag{17}$$

The contained pocket area is presented without derivation and its development can be found in reference 5.

$$\frac{dA}{d\phi} = \frac{4 r_1 r_p sin(\frac{\phi}{T-1})}{T} \tag{18}$$

$$\pm\frac{r}{T-1}\int_{\pi}^{\frac{\pi}{T}} \sqrt{r_P{}^2 + r_1{}^2 - 2.0 r_1 r_P cos(\phi(T/(T-1))} \tag{19}$$

$$-\sqrt{r_P{}^2 + r_1{}^2 - 2.0 r_1 r_P cos(\frac{2\pi}{T-1} - \phi(T/(T-1))}\, d\phi \tag{20}$$

The $\pm$ are the displacements for the external and internal contact respectively. Since the radius of the generating pin, r, has little effect on the flow rate or displacement the same relationship used in the epitrochoidal generation is used. This allows a direct comparison between the external and internal contact.

For direct comparison between gerotors with different lobe ratios the displacement was scaled such that both epitrochoidal and hypotrochoidal gerotors would fit inside a unit circle. Figures 4,5,6, and 7 are plots of the relative displacement and maximum rubbing velocity versus r_p/r_2.

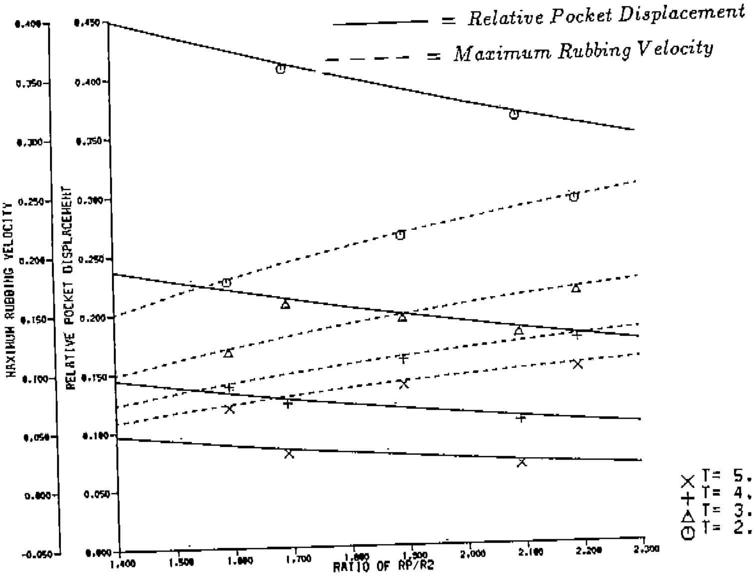

Figure 4: Epitrochoidal generation, external contact, displacement and maximum rubbing velocity

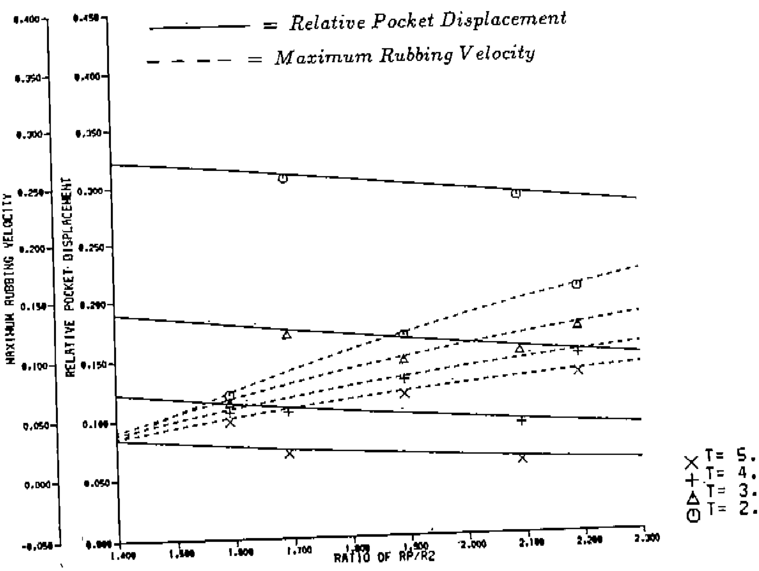

Figure 5: Epitrochoidal generation, internal contact, displacement and maximum rubbing velocity

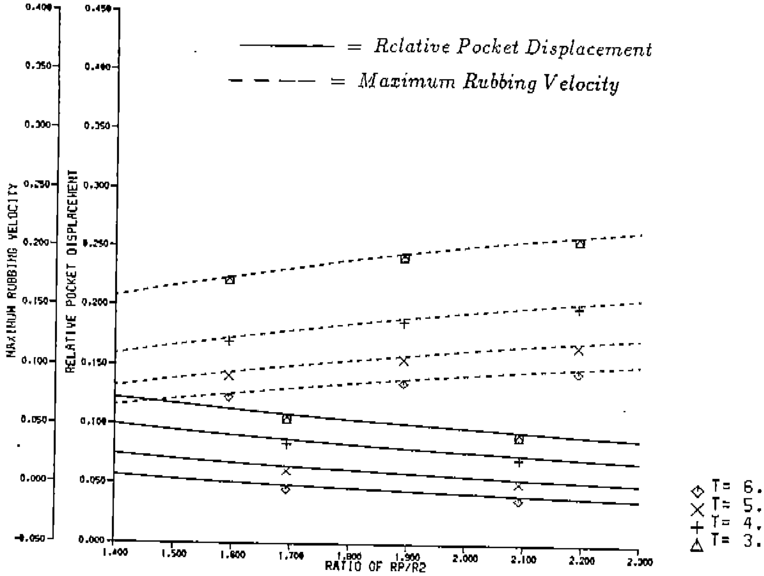

Figure 6: Hypotrochoidal generation, external contact, displacement and maximum rubbing velocity

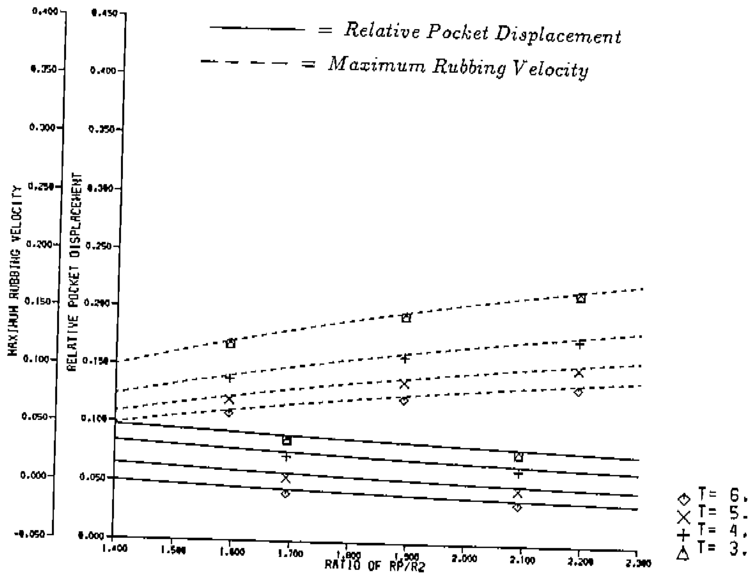

Figure 7: Hypotrochoidal generation, internal contact, displacement and maximum rubbing velocity

CONCLUSIONS

To make a direct comparison between the epitrochoidal and hypotrochoidal generation gerotors, gerotors with the same number of contained pockets will be compared. Since there are T and $T-1$ pockets for epitrochoidal and hypotrochoidal generation respectively, the gear ratios for the equivalent gerotors will not be the same.

It can be seen that the epitrochoidal generation, external contact gerotor has the greatest displacement for a given T and r_p/r_2 ratio. The epitrochoidal generation, internal contact ($with T = 2$) has a displacement of 45% of the external contact. The hypotrochoidal generation, external contact has a displacement of 33% ($with T = 3$) of the epitrochoidal generation, external contact and the hypotrochoidal generation, internal contact has a displacement of 25% of the epitrochoidal generation, external contact. Although the epitrochoidal generation, external contact has the greatest displacement, for a given number of contained pockets and r_p/r_2 ratio, it also has significently higher rubbing velocities than the epitrochoidal generation, internal contact. Both the external and internal contact, hypotrochoidal generation have lower rubbing velocities than the epitrochoidal generation, external contact but the percentage is not significant.

Since the rubbing velocity influences the wear rates and heat transfer rates the epitrochoidal generation, internal contact gerotor may have an advantage over other types of gerotors with its lower rubbing velocity. Further studies are planned to determine if the epitrochoidal generation, internal contact gerotor has a lower contact stress than the external contact for a given displacement.

REFERENCES

[1] Leemhius, R. S. and Soedel, W.,"Vector Loop Analysis of Wankel Compressors and Engines", ASME, 78-DET-1978.

[2] Colbourne, J. R., "The Geometry of Trochoidal Envelopes and their Application in Rotary Pumps", Transactions, CSME, Vol 3, No. 4.

[3] Hall, A. S., "Pin Gearing", ASME Proceedings, Mechanisms Conference, 1968.

[4] Colbourne, J.R. "Gear Shape and Theoretical Flow Rate in Internal Gear Pumps", Transactions CSME, Vol. 3, No. 4.

[5] Beard, J. E., "Kinematic Analysis of Gerotor Type Pumps, Engines, and Compressors", Ph.D. disseration, Purdue University, 1985.

[6] Beard, J. E., Hall, S. S., Soedel, W. "Hypotrochoidal Versus Epitrochoidal Gerotor Type Pumps with Special Attention to Volume Change Ratio and Size", ASME 1987 Design Automation Conference.

[7] Beard, J. E. "Rubbing Velocity of Epitrochoidal Gerotors", 20th Midwesteren Mechanics Conference, Developments in Mechanics.